


Flow-through chronoamperometric sensor based on pillar[3]arene[2]quinone derivative for nitrophenol determination and its application in a model effluent

Dmitry I. Stoikov ^{a *} , Dominika Kappo ^a , Daniil I. Stoikov ^a ,
Dmitry N. Shurpik ^a , Ivan I. Stoikov ^a , Gennady A. Evtugyn ^{ab} 

a: Alexander Butlerov Institute of Chemistry, Kazan (Volga region) Federal University, Kazan 420008, Russia

b: Institute of Chemical Engineering, Ural Federal University, Ekaterinburg 620009, Russia

* Corresponding author: DmIStoikov@kpfu.ru



Abstract

Electrochemical flow-through sensor based on pillar[3]arene[2]quinone (P[3]A[2]Q) derivative was developed. Nitrophenol determination was based on P[3]A[2]Q redox current changes. Also, the shift of cathodic potential was observed compared to nitrophenol reduction current registration directly. Using carbon black (CB) as a matrix for macrocycle implementation provided the sensor stability in the flow when it was applied with a 3D printed flow-through cell. CB and macrocycle were drop casted from the same aliquot providing one-step modifying layer production by the principle of “one-pot synthesis”. The flow-through chronoamperometric sensor designed allowed determining mononitrophenols in the concentration range of 1 nM – 0.1 mM with the limit of detection (LOD) of 0.5 nM. The linear concentration range of 10 nM – 0.1 mM with LOD of 2 nM was obtained for 2,4-dinitrophenol, 2,6-dinitrophenol and 2,4,6-trinitrophenol. The sensor proposed was tested with a model effluent sample, and sufficient recovery about 98±1% was obtained.

Key findings

- Electrochemical sensor based on carbon black and pillar[3]arene[2]quinone for nitrophenol determination was developed.
- Pillar[3]arene[2]quinone engages with nitrophenols on the “host-guest” interaction principle, which allowed to shift the cathodic potential of nitrophenol determination.
- Low limits of detection allow using the sensor for eco-monitoring of nitrophenols in a real sample.

© 2024, the Authors. This article is published in open access under the terms and conditions of the Creative Commons Attribution (CC BY) license (<http://creativecommons.org/licenses/by/4.0/>).

1. Introduction

Electrochemical sensors are powerful analytical equipment due to their portability, mobility and affordable cost. Their high sensitivity and selectivity account for their wide usage in environment monitoring and clinical diagnostics, whereas there is a possibility to use them both in laboratory and in point-of-care testing [1].

Electrochemical sensors response is a result of electrochemical conversion of analyte or a redox mediator on the transducer interface into a readable electric signal.

Analytical characteristics such as selectivity and sensitivity are strongly dependent on microstructure and properties of the electrode modifying coating [2], so the nanostructured materials are commonly used to improve

the analytical characteristics of the sensors developed [3]. The inclusion of macrocyclic compounds such as cyclodextrin, calix[n]arene, curcubituril, etc., into modifying layer is a promising approach in the field of electrochemical sensor development. These compounds have the unique size of macrocycle cavities and some specific properties that allow creating novel kinds of selective sensors. Outstanding features of macrocycles found their application in various supramolecular systems such as liquid crystals [4], mechanically interlocked molecules [5], metallorganic backbone structures [6], supramolecular polymers [7–9], drug delivery systems [10, 11], cell bioimaging agents [12], transmembrane ion channels [13], and molecular glue [14]. Supramolecular “bottom-up” assembly provides an efficient tool for multifunctional hybrid system design by including the

Accompanying information

Article history

Received: 25.10.24

Revised: 05.11.24

Accepted: 05.11.24

Available online: 19.11.24


Keywords


Flow-through analysis; Pillar[3]arene[2]quinone; Nitrophenol determination; Electrochemical sensor; Macrocyces

Funding

This work was supported by the Russian Science Foundation (grant no. 22-13-00070 <https://rscf.ru/en/project/22-13-00070>).

Supplementary information

Supplementary materials:  **READ**

Transparent peer review:  **READ**

Sustainable Development Goals



individual functional components through the non-covalent interactions. Among them “host-guest” molecular recognition becomes more attractive for the researchers. The reason is the opportunity to bind two or more molecules in a simple and reversible way, which allows to design some new supramolecular structures [15–17]. It confirms the great promise of using macrocycles for sensor devices development.

Pillar[n]arenes are among the most interesting compounds to include into electrochemical sensors assembly. First obtained by T. Ogoshi et al. [18], they represent a novel class of supramolecular compounds [19]. They combine some characteristics of other “host-guest” systems such as highly symmetrical column structure as in cucurbiturils, rich π -electron density in aromatic cavity as in calix[n]arenes and a lot of hydroxyl groups at the rims typical for highly functionalized cyclodextrins [20]. Previously, the functionalized pillar[n]arenes were used as a part of solubilizers [21], gelatinization agents [22], sorbents [23], target drug delivery systems [24], OLED-devices [25] and transmembrane ion channels [26].

Nowadays, the number of studies using pillar[n]arenes as the sensor modifiers is limited, but the idea of their application is an essential and promising one due to the unique properties of their structure [20]. In particular, pillar[5]arene and its derivatives exhibit sufficient electrochemical activity. These compounds were used for a selective determination of organic phosphorus and carbamate pesticides [27], neuromediators [28, 29], paraquat [30], hemoglobine [3], metal ions [31], chiral substances [32], caffeic acid [33], aflatoxine M1 [34], hydrogen peroxide, uric acid [35] and DNA damage discrimination [36]. Thus, pillar[5]arenes (especially those functionalized with different groups) are promising agents which can be used in the development of devices for determining a wide range of compounds.

Nitrophenols represent one of the most important groups of environment pollutants. They are widely used in such industrial areas as production of plastics, paints, insecticides and explosives [37]. They tend to accumulate in water and soil, so they are high priority pollutants of the environment endangering people health [38]. At the moment there are different approaches of chemical analysis used for nitrophenol determination: high-performance liquid chromatography [39], UV-vis spectroscopy [40], fluorescence spectroscopy [41], capillary electrophoresis [42] and electrochemical devices [43]. The latter are the most convenient and exhibit high sensitivity and reproducibility [38] along with an opportunity to carry out the “on-site” analysis [44]. All of these advantages together provide an accurate determination of nitrophenols for ecomonitoring aims.

In this work we suggested mononitrophenols, 2,4-dinitrophenol, 2,6-dinitrophenol and 2,4,6-trinitrophenol determination through redox peak currents of pillar[5]arene quinone derivative. This derivative engages with nitrophenols on the principle “host-guest” interaction which allows shifting the cathodic potential of nitrophenol determination compared to their own reduction peaks registration. The

electrochemical sensor based on pillar[5]arene quinone derivative demonstrates a high level of sensitivity towards all the nitrophenols studied. Both cyclic voltammetry and chronoamperometry were applied for the evaluation of analyte determination parameters. The flow-through chronoamperometric determination was carried out with a 3D printed electrochemical cell made of polylactic acid. This material meets all the requirements of three-dimension printing. In addition, biodegradability of this substance, its compatibility with biopolymers, low cost, and sufficient treatment accuracy make polylactic acid an appropriate material for flow-through cell production.

2. Materials and methods

2.1. Reagents

4,8,14,18,23,26,28,31,32,34-decakis(2'-bromethoxy)-pillar[5]arene (pillar[3]arene[2]quinone, P[3]A[2]Q) (Figure 1) was synthesized according to ref [45].

Carbon black (CB) N220 was purchased from Cabot (Ravenna, Italy). Prior to its use, 1.0 mg of CB was mixed with 0.25 mL of concentrated nitric acid and 0.75 mL of concentrated sulphuric acid followed by ultrasonication for 60 min. The sediment was spinned off, rinsed and dried at 60 °C. The oxidized CB was ultrasonicated in 1.5 mL of propylene carbonate for 2 h to obtain 0.66 mg/mL working solution. The P[3]A[2]Q exact mass was dissolved in CB 0.66 mg/mL suspension up to 10 mM concentration followed by ultrasonication for 2 h in the case of modifier “one-pot synthesis”.

All the other reagents were of analytical grade and did not require any additional purification. The working solutions were prepared using deionized water Millipore-Q (Simplicity®, Merck-Millipore, Mosheim, France).

All the measurements were carried out in the Britton-Robinson buffer (BRB) consisting of 40 mM acetic acid, 40 mM phosphoric acid, 40 mM boric acid and 50 mM potassium sulphate.

The model solution of effluents contained 0.04 M H_3PO_4 , 0.04 M H_3BO_3 , 0.04 M CH_3COOH , 0.05 M NaSO_4 , 0.41 mM CaCl_2 , 0.26 mM MgCl_2 , 93 μM NH_4Cl , 0.27 mM KOH [46] spiked with *m*-nitrophenol was used for sensor aprobation in a real sample.

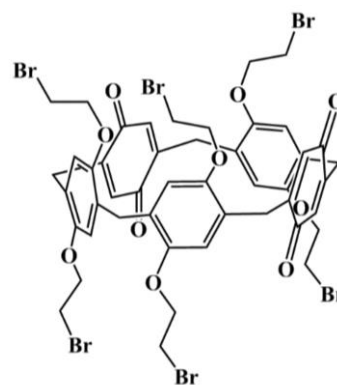


Figure 1 Chemical structure of P[3]A[2]Q.

2.2. Screen-printed carbon electrodes (SPCEs) modification

SPCEs were produced utilizing a printer DEC 248 (Dec, London, England) on Lomond PE DS Laser Film (thickness 125 μm , Lomond Trading Ltd., Douglas, Isle of Man) through step-by-step coating of 4 layers. They were: the conductive polymeric PSP-2 silver tracks (Delta-Paste, Moscow, Russia), silver paste layer for pseudo-reference electrode fabrication (polymeric paste Ag/AgCl PSCP-1, Delta-Paste, Moscow, Russia), tracks of carbon/graphite paste C2030519P4 as a counter and a working electrode (Gwent group, Pontypool, the UK) and an isolating layer (paste D21440114D5 Gwent group, Pontypool, the UK). Every layer was hardened at 80 $^{\circ}\text{C}$. The geometric area of working electrode was equal to 3.8 mm^2 .

The working electrode modification was carried out by drop casting of 1 μL suspension consisted of 0.66 mg/mL CB and 10 mM P[3]A[2]Q in propylene carbonate followed by drying in the oven at 100 $^{\circ}\text{C}$.

2.3. Flow-through cells fabrication

The flow-through cell was designed using Wanhao Duplicator 9/300 (Jinhua Wanhao Spare Parts, Wanhao, China) with one extruder (nozzle diameter 0.3 mm) from the poly(lactic acid) filaments. The layer thickness was 0.1 mm with a printing rate 700 mm per second at 220 $^{\circ}\text{C}$. The 3D model of the flow-through cell designed is presented at Figure S1. The dimensions of the cells were 2.4x4.4x2.7 cm . The volume of a replaceable inner camera of the flow-through cell was 10 μL .

Multi-mode potentiostat BioStat (ESA Bioscience Inc., Chelmsford, Massachusetts, USA) was used for chronoamperometric experiments. Voltammetric investigations were carried out with potentiostat-galvanostat CHI 660E (CH Instruments, Austin, Texas, the USA).

3. Results and Discussion

3.1. Electrochemical behaviour of coating based on CB and P[3]A[2]Q

Pillar[5]arenes [47] and their derivatives [48] were successfully used as electron transfer mediators in electrochemical sensor and biosensor development. However, these compounds have some disadvantages, for example, electrode coating based on pillar[5]arene can lose its electrochemical activity over time due to intramolecular bounds formation [49]. Pillarquinones are devoid of this disadvantage and demonstrate the tendency to quasi-reversible redox conversion that is not complicated by intramolecular bounds appearance [45].

Pillar[5]arenes as a modifying electrode coating are often used together with carbon nanomaterials to prevent surface inactivation caused by chemisorption of intermediate oxidation products [50]. In this work P[3]A[2]Q was applied simultaneously with CB from a single aliquot in one-

step protocol that was possible because propylene carbonate was used as a solvent. Implementation of CB into the coating content led to 2.5 times increase in the P[3]A[2]Q redox peak height (Figure 2).

The surface activation after the modifier deposition on the electrode was carried out by tenfold scanning of the potential. Redox peak currents grew during five consecutive cycles of potential scanning followed by the stabilization of the peak currents (Figure 3).

The nature of the redox signals and P[3]A[2]Q electrochemical conversion was discussed in details in the previous studies [45]. The proposed mechanism of reversible reduction and oxidation of quinone fragments in P[3]A[2]Q molecules is presented in Scheme 1.

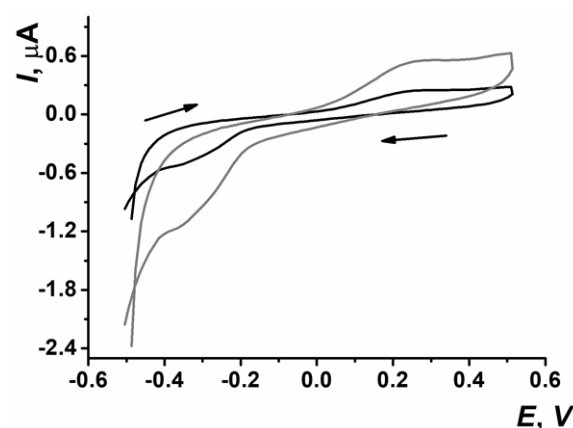


Figure 2 Voltammograms recorded on SPCEs modified with P[3]A[2]Q only (black) and CB with P[3]A[2]Q (grey). Cyclic voltammetry, BRB, pH 7.0, 0.1 V/s.

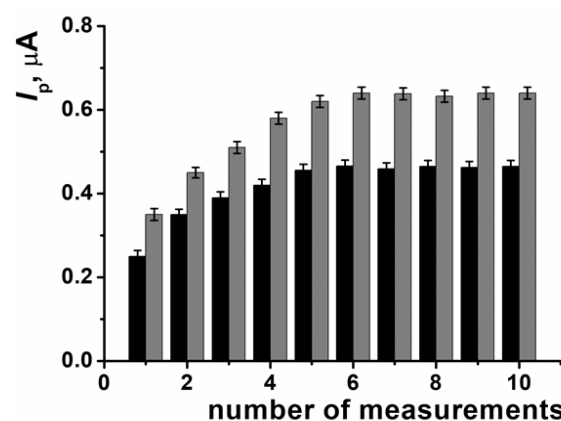
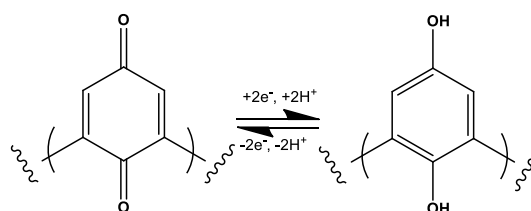


Figure 3 Anodic (black) and cathodic (grey) peak currents recorded on SPCEs modified with CB and P[3]A[2]Q depending on number of measurements. Average \pm S.D. for five individual sensors prepared from the set of equal reagents. Cyclic voltammetry, BRB, pH 7.0, 0.1 V/s.



Scheme 1 The proposed mechanism of reversible reduction and oxidation of quinone fragments in P[3]A[2]Q molecules.

3.2. Voltammetric determination of nitrophenols

The response changes of the coating based on P[3]A[2]Q in presence of *o*-nitrophenol, *m*-nitrophenol, *p*-nitrophenol, 2,4-dinitrophenol, 2,6-dinitrophenol, 2,4,6-trinitrophenol were investigated. Redox peak currents of P[3]A[2]Q increased with nitrophenol concentration. Probably, the interaction between P[3]A[2]Q and nitrophenols occurs through the “host-guest” mechanism [51]. Electrochemical determination of nitrophenols by P[3]A[2]Q peak currents has the advantage compared to the other common methods. This advantage is based on intrinsic nitrophenol reduction currents. Here, the redox peaks were observed at much lower potentials in the range from -0.8 to -0.6 V [38, 52, 53] compared to P[3]A[2]Q oxidation peak potential in the area close to 0.25 V. For all mononitrophenols the morphology and the peak current values were quite similar. The typical cyclic voltammograms for *m*-nitrophenol determination are presented in Figure 4a.

Voltammetric determination of nitrophenols through redox peak currents of P[3]A[2]Q allows the quantification of mononitrophenols in the range from 10 nM to 0.1 mM with the limit of detection (LOD) of 5 nM. The LOD value was calculated for $S/N = 3$ criteria. The example of calibration curve for *m*-nitrophenol is presented in Figure 4b, the calibration curves for all *mono*-nitrophenols are presented in Figure S2.

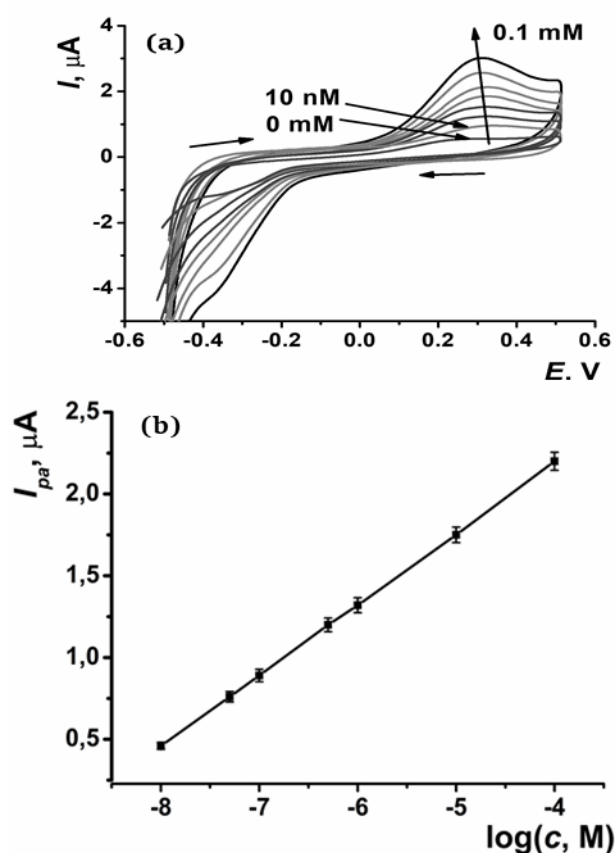


Figure 4 Voltammograms of SPCEs modified with CB and P[3]A[2]Q in the presence of different concentrations of *m*-nitrophenol (a); calibration curve of *m*-nitrophenol determination. Average \pm S.D. for five individual sensors prepared from the set of equal reagents (b). BRB, pH 7.0, 0.1 V/s.

The voltammograms of 2,4-dinitrophenols, 2,6-dinitrophenols and 2,4,6-trinitrophenols were recorded in the same way. The current peak morphology and the values were very similar for these three compounds. But compared to voltammograms recorded for *m*-nitrophenols, the oxidation peak for di- and trinitrophenols was less pronounced. The difference in the sensor response and shape of the peaks for mono-, di-, and trinitrophenols is likely due to steric constraints within di- and tri-nitro compound incorporation into the cavity of P[3]A[2]Q. It is attributed to the number of substituents and, consequently, size. The typical cyclic voltammograms for 2,4-dinitrophenol determination are presented in Figure 5a.

The P[3]A[2]Q redox peak currents allow determining 2,4-dinitrophenol, 2,6-dinitrophenol and 2,4,6-trinitrophenols in the range from 0.1 μ M to 0.1 mM using the voltammetric approach. The LOD was equal to 50 nM calculated for $S/N = 3$ criteria. The example of calibration curve for 2,4-dinitrophenol is presented in Figure 5b; the calibration curves for di- and trinitrophenols are presented in Figure S3.

The linear regression equation parameters for each type of the compounds studied are presented in Table 1.

3.3. Chronoamperometric nitrophenol detection

The approach introduced was further used for chronoamperometric sensor development based on 3D printed flow-throw system and SPCE modified with CB and P[3]A[2]Q.

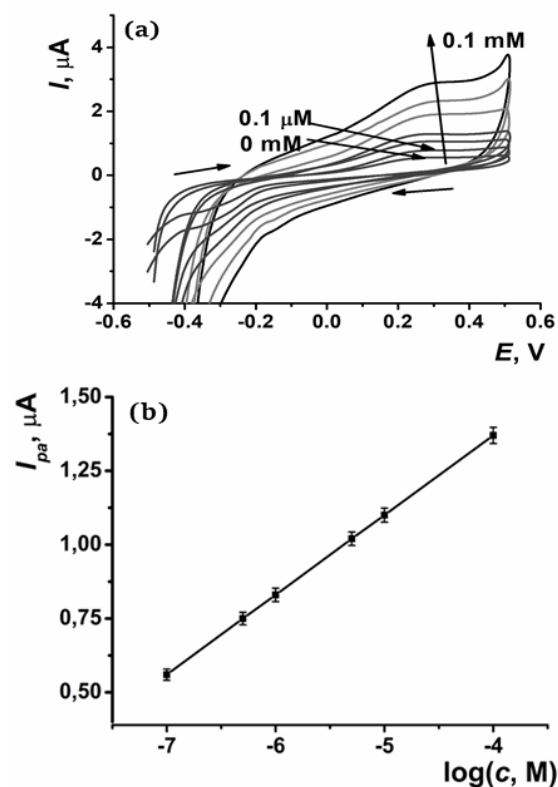


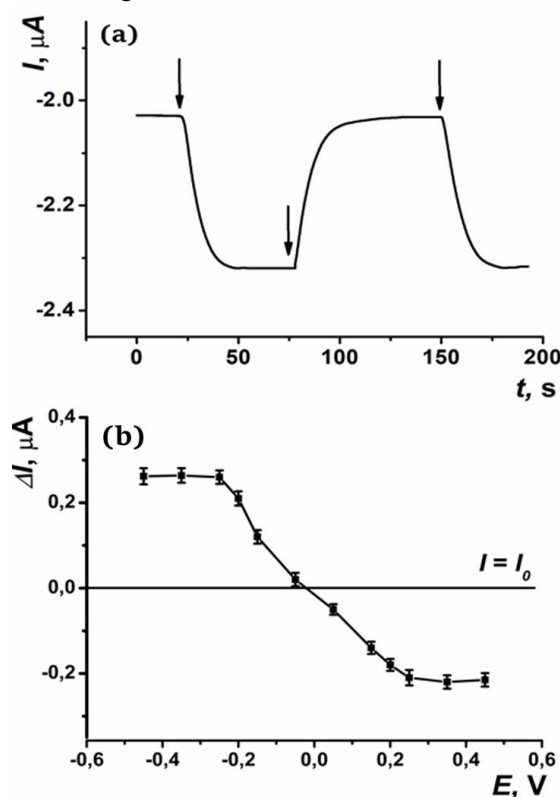
Figure 5 Voltammograms recorded on SPCEs modified with CB and P[3]A[2]Q in the presence of different concentrations of 2,4-dinitrophenol (a); calibration curve of 2,4-dinitrophenol determination (b). Average \pm S.D. for five individual sensors prepared from the set of equal reagents. BRB, pH 7.0, 0.1 V/s.

Table 1 Linear regression equation parameters for the nitrophenols studied with voltametric approach on SPCE covered with CB and P[3]A[2]Q.

| Analyte | $y = a + bx$ $\Delta(I, \mu A) = a + b \cdot \log(c, M)$ | R^2 |
|----------------------|---|--------|
| p-nitrophenol | $I, \mu A = (3.87 \pm 0.02) + (0.429 \pm 0.002) \cdot \log(c, M)$ | 0.9998 |
| m-nitrophenol | $I, \mu A = (3.92 \pm 0.01) + (0.433 \pm 0.002) \cdot \log(c, M)$ | 0.9999 |
| o-nitrophenol | $I, \mu A = (3.96 \pm 0.02) + (0.437 \pm 0.003) \cdot \log(c, M)$ | 0.9997 |
| 2,4-dinitrophenol | $I, \mu A = (2.45 \pm 0.01) + (0.264 \pm 0.002) \cdot \log(c, M)$ | 0.9998 |
| 2,6-dinitrophenol | $I, \mu A = (2.40 \pm 0.02) + (0.269 \pm 0.002) \cdot \lg(c, M)$ | 0.9998 |
| 2,4,6-trinitrophenol | $I, \mu A = (2.49 \pm 0.03) + (0.275 \pm 0.004) \cdot \log(c, M)$ | 0.9997 |

The flow of buffer or analyte solution was sequentially passed through the electrochemical cell, and the current shift was recorded. The chronoamperometric signal was quite similar for such mononitrophenols as *o*-nitrophenol, *m*-nitrophenol, and *p*-nitrophenol. Another group of compounds with similar signal was formed from di- and trinitrophenols: 2,4-dinitrophenol, 2,6-dinitrophenol, and 2,4,6-trinitrophenol.

The sensor signal (ΔI) for all nitrophenols studied was defined as a difference between the currents measured in absence (I_0) and in presence (I) of nitrophenol in the flow. Dynamic sensor response for *m*-nitrophenol as an example is shown in Figure 6a.

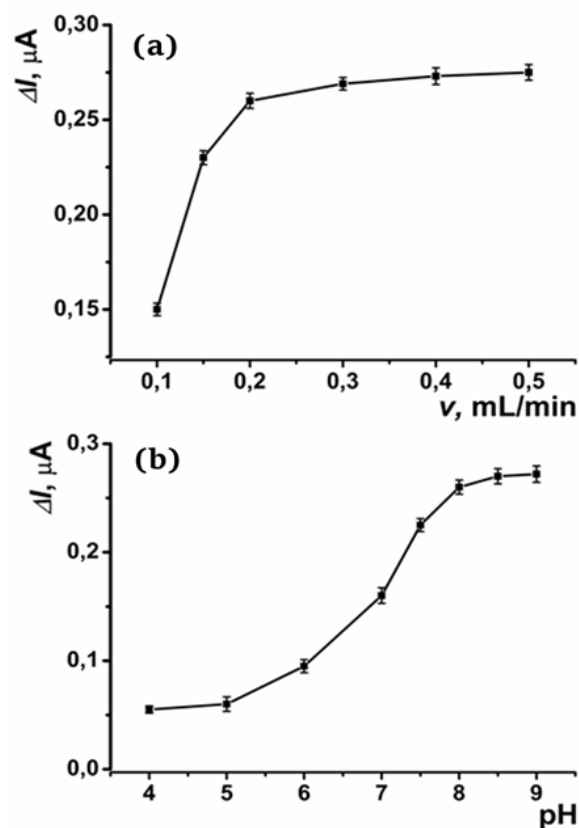
**Figure 6** Chronoamperometric sensor response at -0.25 V (a) and current shift dependence on polarization potential on SPCE modified with CB and P[3]A[2]Q in presence of $10 \mu M$ of *m*-nitrophenol (b). Arrows indicate the flow switching from buffer solution to *m*-nitrophenol solution and back. Average \pm S.D. for five individual sensors prepared from the set of equal reagents. Chronoamperometry, BRB, pH 8.0, flow rate 0.2 mL/min.

The chronoamperometric response was observed both at negative and positive potentials; however, the maximal response was achieved at -0.25 V. The typical current shift dependence on the polarization potential for *m*-nitrophenol is presented in Figure 6b.

To get the highest response value, the flow rate of 0.2 mL/min and the pH value of 8.0 should have been used for all nitrophenols. The current shift dependences on flow rate and pH value for *m*-nitrophenol are presented in Figure 7. This type of regularity was observed for all of nitrophenols investigated.

The signal increased with pH value in the range from 2.0 to 6.0 with a sharp increase in the area of 6.0–8.0. After the pH value reached 8.0, the signal stabilization was observed. This behavior can be explained by alternative oxidation of quinone groups by dissolved oxygen. The oxygen reactivity is higher in alkaline medium.

The sensors developed allowed determining various mononitrophenols at concentrations from 1 nM to 0.1 mM with LOD of 0.5 nM, according to the $S/N = 3$ criteria. As for 2,4-dinitrophenol, 2,6-dinitrophenol, and 2,4,6-trinitrophenol, the linear range was from 10 nM to 0.1 mM with LOD equal to 2 nM, calculated for $S/N = 3$ criteria. Calibration curves for *m*-nitrophenol and 2,4-dinitrophenol as the examples are shown in Figure 8, calibration curves for all the compounds are presented in Figure S4 and Figure S5.

**Figure 7** Current shift dependences on flow rate (a) and pH value (b) for SPCEs modified with CB and P[3]A[2]Q in presence of $10 \mu M$ of *m*-nitrophenol at -0.25 V. Average \pm S.D. for five individual sensors prepared from the set of equal reagents. Chronoamperometry, BRB, (a) pH 8.0, (b) flow rate 0.2 mL/min.

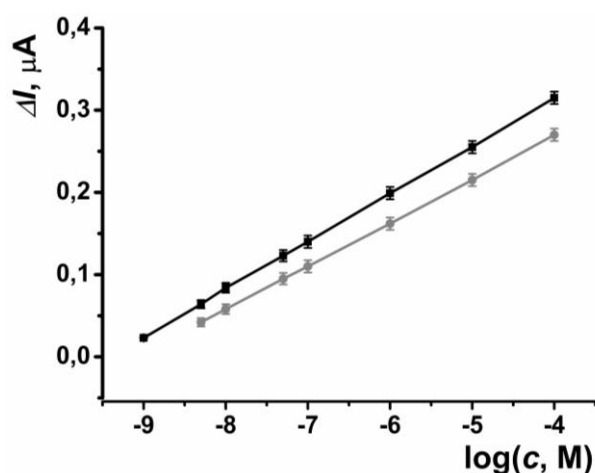


Figure 8 Calibration curves of *m*-nitrophenol (black) and 2,4-dinitrophenol (grey) on SPCEs modified with CB and P[3]A[2]Q. Average \pm S.D. for five individual sensors prepared from the set of equal reagents. Chronoamperometry, BRB, pH 8.0, flow rate 0.2 mL/min, -0.25 V.

Analytical characteristics of the mono-, di-, and trinitrophenols with the flow-through system are presented in Table 2.

The 3D printed flow-through system using SPCE modified with CB and P[3]A[2]Q allows performing up to 40 measurements per hour on the same electrode.

In spite of the durable effect of the flow in the flow-through system, there were no significant changes in the properties of modifying layer on SPCEs. This can be explained by the high stability of the coating based on CB combined with P[3]A[2]Q.

Analytical characteristics of the nitrophenol determination on the sensors developed are presented in Table 3 and are comparable or better than ones for the other electrochemical sensors previously reported in the literature.

The interfering effect of the components of model effluent solution on *m*-nitrophenol chronoamperometric determination parameters was assessed (Table 4).

Table 2 Analytical characteristics of the various nitrophenols determination using the flow-through system and SPCEs modified with CB and P[3]A[2]Q.

| Analyte | $y = a + bx$ | R^2 |
|----------------------|---|--------|
| | $\Delta(I, \mu A) = a + b \cdot \log(c, M)$ | |
| p-nitrophenol | $\Delta(I, \mu A) = (0.557 \pm 0.004) + (0.0579 \pm 0.0003) \cdot \log(c, M)$ | 0.9998 |
| m-nitrophenol | $\Delta(I, \mu A) = (0.549 \pm 0.02) + (0.0584 \pm 0.0003) \cdot \log(c, M)$ | 0.9999 |
| o-nitrophenol | $\Delta(I, \mu A) = (0.534 \pm 0.03) + (0.0592 \pm 0.0004) \cdot \log(c, M)$ | 0.9998 |
| 2,4-dinitrophenol | $\Delta(I, \mu A) = (0.479 \pm 0.002) + (0.0527 \pm 0.0003) \cdot \log(c, M)$ | 0.9998 |
| 2,6-dinitrophenol | $\Delta(I, \mu A) = (0.482 \pm 0.002) + (0.0534 \pm 0.0004) \cdot \log(c, M)$ | 0.9997 |
| 2,4,6-trinitrophenol | $\Delta(I, \mu A) = (0.475 \pm 0.003) + (0.0519 \pm 0.002) \cdot \log(c, M)$ | 0.9997 |

The model sample of effluent contained 0.04 M H_3PO_4 , 0.04 M H_3BO_3 , 0.04 M CH_3COOH , 0.05 M Na_2SO_4 , 0.41 mM $CaCl_2$, 0.26 mM $MgCl_2$, 93 μM NH_4Cl and 0.27 mM KOH . After 100-fold dilution of the sample with working buffer solution the recovery obtained was 98 %. Since the maximum permissible concentration level of nitrophenols in the effluents was in micromolar range [72], the sensor developed can provide a reliable determination of the ecotoxicant in natural reservoirs.

4. Limitations

There are no special limitations in our study.

5. Conclusion

The electrochemical sensor based on SPCE modified with CB and P[3]A[2]Q was developed. The device demonstrated high sensitivity towards a group of nitrophenols. Voltammetric measurements allowed observing the increase of P[3]A[2]Q own redox peaks in presence of nitrophenols, which can be attributed to their possible “host-guest” interaction. This fact helped to carry out the chronoamperometric measurements at the potential of -0.25 V which is much higher than the cathodic potential of nitrophenols direct reduction recorded at the range $-0.8 \dots -0.6$ V. The flow-through chronoamperometric approach provided the possibility of mononitrophenols and 2,4-dinitrophenol, 2,6-dinitrophenol and 2,4,6-trinitrophenol determination in the concentration ranges from 1.0 nM to 0.1 mM with LOD of 0.5 nM and from 10 nM to 0.1 mM with LOD of 2 nM, respectively.

The electrochemical sensor suggested has a low cost and a simple assembly. Thus, all the modifying components were casted from a single aliquot that allowed us to produce the modifying coating in one step using “one-pot synthesis” principle. Beside this, using CB as a matrix for P[3]A[2]Q implementation into the electrode coating helped to maintain its mechanical stability during the flow-through measurements. This feature provides multiple (up to 40 per hour) measurements on a single sensor.

The recovery value of 100-fold diluted sample of model effluent was $98 \pm 1\%$ for *m*-nitrophenol. In addition, low limits of detections and micromolar permissible concentration levels allow using the sensor developed for eco-monitoring of nitrophenols in natural water. The advantage of flow-through analysis methods is primarily provided by the large number of analyzed samples over a period of time. Additionally, the use of 3D printed flow-through cell has such advantages as easy replacement of individual components, extremely low manufacturing cost, biocompatibility and biodegradability.

Table 3 Comparison of the electrochemical characteristics of the sensors developed with other electrochemical sensors for nitrophenol determination described in literature.

| Sensor content | Detection mode | Concentration range, M | LOD, M | Ref. |
|---|------------------|---|----------------------|-----------|
| <i>o</i> -nitrophenol | | | | |
| GCE ^a /graphene nanosheets, functionalized with β -cyclodextrins | DPV ^b | $5.0 \cdot 10^{-6}$ – $4.0 \cdot 10^{-4}$ | $3.0 \cdot 10^{-7}$ | [54] |
| GCE/GO ^c /poly(ethyleneimine) dendrimer | DPV | $5.0 \cdot 10^{-6}$ – $1.55 \cdot 10^{-4}$ | $1.0 \cdot 10^{-7}$ | [55] |
| GCE/cyclodextrin/RGO ^d , functionalized with chitosan | DPV | $1.2 \cdot 10^{-7}$ – $4.0 \cdot 10^{-5}$ | $1.8 \cdot 10^{-8}$ | [56] |
| SPCE/(CB + P[3]A[2]Q) | CV ^e | $1.0 \cdot 10^{-8}$ – $1 \cdot 10^{-4}$ | $5.0 \cdot 10^{-9}$ | This work |
| SPCE/(CB + P[3]A[2]Q) | CA ^f | $1.0 \cdot 10^{-9}$ – $1 \cdot 10^{-4}$ | $5.0 \cdot 10^{-10}$ | This work |
| <i>m</i> -nitrophenol | | | | |
| CPE ^g / β -cyclodextrin, mesoporous Si | CV | $2.0 \cdot 10^{-7}$ – $1.4 \cdot 10^{-6}$ | $5.0 \cdot 10^{-8}$ | [57] |
| GCE/macroporous carbon, amino-bridged organic poly-calix[4]arenes | DPV | $1.0 \cdot 10^{-6}$ – $4.0 \cdot 10^{-4}$ | $1.22 \cdot 10^{-7}$ | [58] |
| GCE/magnetite-PtNPs ^h , stabilized with 3-n-propyl-4-picoline | DPV | $1.0 \cdot 10^{-7}$ – $1.5 \cdot 10^{-6}$ | $4.5 \cdot 10^{-8}$ | [59] |
| SPCE/(CB + P[3]A[2]Q) | CV | $1.0 \cdot 10^{-8}$ – $1 \cdot 10^{-4}$ | $5.0 \cdot 10^{-9}$ | This work |
| SPCE/(CB + P[3]A[2]Q) | CA | $1.0 \cdot 10^{-9}$ – $1 \cdot 10^{-4}$ | $5.0 \cdot 10^{-10}$ | This work |
| <i>p</i> -nitrophenol | | | | |
| GCE/Ni/N-doped carbon nanocomposite | DPV | $6.0 \cdot 10^{-8}$ – $1.0 \cdot 10^{-4}$ | $4.0 \cdot 10^{-9}$ | [60] |
| GCE/Cr-MOF ⁱ NPs | DPV | $2.0 \cdot 10^{-6}$ – $5.0 \cdot 10^{-4}$ | $7.0 \cdot 10^{-7}$ | [61] |
| GCE/GO | DPV | $1.0 \cdot 10^{-7}$ – $1.2 \cdot 10^{-4}$ | $2.0 \cdot 10^{-8}$ | [62] |
| SPCE/(CB + P[3]A[2]Q) | CV | $1.0 \cdot 10^{-8}$ – $1 \cdot 10^{-4}$ | $5.0 \cdot 10^{-9}$ | This work |
| SPCE/(CB + P[3]A[2]Q) | CA | $1.0 \cdot 10^{-9}$ – $1 \cdot 10^{-4}$ | $5.0 \cdot 10^{-10}$ | This work |
| 2,4-dinitrophenol | | | | |
| GCE/MIP ^j /GO | CV | $1.0 \cdot 10^{-6}$ – $1.5 \cdot 10^{-3}$ | $1.0 \cdot 10^{-6}$ | [63] |
| GCE/C ₃ N ₄ /V ₂ O ₅ | CV | $1.0 \cdot 10^{-8}$ – $1.0 \cdot 10^{-4}$ | $3.3 \cdot 10^{-9}$ | [64] |
| GCE/RuO ₂ NPs-decorated V ₂ O ₅ nanoflakes | DPV | $5.0 \cdot 10^{-9}$ – $3.5 \cdot 10^{-6}$ | $1.07 \cdot 10^{-9}$ | [65] |
| SPCE/(CB + P[3]A[2]Q) | CV | $1.0 \cdot 10^{-7}$ – $1.0 \cdot 10^{-4}$ | $5.0 \cdot 10^{-8}$ | This work |
| SPCE/(CB + P[3]A[2]Q) | CA | $1.0 \cdot 10^{-8}$ – $1.0 \cdot 10^{-4}$ | $2.0 \cdot 10^{-9}$ | This work |
| 2,6-dinitrophenol | | | | |
| PGE/AgNPs/chitosan/SrSnO ₃ nanocomposite | DPV | $1.5 \cdot 10^{-6}$ – $1.35 \cdot 10^{-5}$ | $1.8 \cdot 10^{-7}$ | [66] |
| GCE/poly(Congo red) | CV | $5.0 \cdot 10^{-7}$ – $6.5 \cdot 10^{-5}$ | $1.0 \cdot 10^{-7}$ | [67] |
| GCE/ ZnO-PbO microstructures | DPV | $3.23 \cdot 10^{-6}$ – $1.67 \cdot 10^{-5}$ | $2.95 \cdot 10^{-6}$ | [68] |
| SPCE/(CB + P[3]A[2]Q) | CV | $1.0 \cdot 10^{-7}$ – $1.0 \cdot 10^{-4}$ | $5.0 \cdot 10^{-8}$ | This work |
| SPCE/(CB + P[3]A[2]Q) | CA | $1.0 \cdot 10^{-8}$ – $1.0 \cdot 10^{-4}$ | $2.0 \cdot 10^{-9}$ | This work |
| 2,4,6-trinitrophenol | | | | |
| Au electrode/carbon quantum dots | DPV | $5.0 \cdot 10^{-10}$ – $5.0 \cdot 10^{-6}$ | $3.5 \cdot 10^{-10}$ | [69] |
| PGE/MIP/RGO/polypyrrol | DPV | $1.0 \cdot 10^{-5}$ – $1.0 \cdot 10^{-3}$ | $1.4 \cdot 10^{-6}$ | [70] |
| GCE/1,3,5-benzotricarboxylic acid/RGO | DPV | $2.0 \cdot 10^{-7}$ – $1.0 \cdot 10^{-5}$ | $1.0 \cdot 10^{-7}$ | [71] |
| SPCE/(CB + P[3]A[2]Q) | CV | $1.0 \cdot 10^{-7}$ – $1.0 \cdot 10^{-4}$ | $5.0 \cdot 10^{-8}$ | This work |
| SPCE/(CB + P[3]A[2]Q) | CA | $1.0 \cdot 10^{-8}$ – $1.0 \cdot 10^{-4}$ | $2.0 \cdot 10^{-9}$ | This work |

^a GCE – glassy carbon electrode;^b DPV – differential pulse voltammetry;^c GO – graphene oxide;^d RGO – reduced graphene oxide;^e CV – cyclic voltammetry;^f CA – chronoamperometry;^g CPE – carbon paste electrode;^h NPs – nanoparticles;ⁱ Cr-MOF – chrome metal-organic framework;^j MIP – molecularly imprinted polymers.

Table 4 Chronoamperometric recovery of *m*-nitrophenol in a model effluent sample.

| Model effluent sample | <i>m</i> -nitrophenol, μM | | Sr | Recovery, % |
|-----------------------|--------------------------------------|---------------|-------|-------------|
| | Added | Found | | |
| No dilution | | 3.5 \pm 0.2 | 0.045 | 35 \pm 2 |
| Dilution 1:10 | 10 | 6.7 \pm 0.1 | 0.015 | 67 \pm 1 |
| Dilution 1:100 | | 9.8 \pm 0.1 | 0.010 | 98 \pm 1 |

Supplementary materials

This manuscript contains supplementary materials, which are available on the corresponding online page.

Data availability statement

The raw/processed data required to reproduce the above findings cannot be shared at this time as the data also forms part of an ongoing study.

Acknowledgments

None.

Author contributions

Conceptualization: G.A.E., D.I.S., I.I.S.
 Data curation: D.K.
 Formal Analysis: D.I.S., D.K., Da.I.S.
 Funding acquisition: G.A.E., D.N.S., I.I.S.
 Investigation: D.I.S., Da.I.S.
 Methodology: D.I.S., D.N.S., G.A.E.
 Project administration: G.A.E.
 Resources: G.A.E., I.I.S.
 Software: Da.I.S., D.I.S.
 Supervision: G.A.E.
 Validation: Da.I.S., D.K., D.N.S.
 Visualization: D.I.S.
 Writing – original draft: D.I.S.
 Writing – review & editing: D.K.

Conflict of interest

The authors declare no conflict of interest.

Additional information

Author IDs:

Dmitry I. Stoikov, Scopus ID [57208315826](#);
 Dominika Kappo, Scopus ID [57204267835](#);
 Dmitry N. Shurpik, Scopus ID [56399350900](#);
 Ivan I. Stoikov, Scopus ID [6602887534](#);
 Gennady A. Evtugyn, Scopus ID [6602814884](#).

Website:

Kazan (Volga region) Federal University, <https://kpfu.ru/Eng/>.

References

- Zhang W, Wang R, Luo F, Wang P, Lin Z. Miniaturized electrochemical sensors and their point-of-care applications. *Chin Chem Lett.* 2020;31(3):589–600. doi:[10.1016/j.cclet.2019.09.022](#)
- Liu Z, Du J, Qiu C, Huang L, Ma H, Shen D, Ding Y. Electrochemical sensor for detection of p-nitrophenol based on nanoporous gold. *Electrochem Commun.* 2009;11(7):1365–1368. doi:[10.1016/j.elecom.2009.05.004](#)
- Wang J, Zhou L, Bei J, Xie M, Zhu X, Chen T, Wang X, Du Y, Yao Y. An specific photoelectrochemical sensor based on pillar[5]arenes functionalized gold nanoparticles and bismuth oxybromide nanoflowers for bovine hemoglobin recognition. *J Colloid Interface Sci.* 2022;620:187–198. doi:[10.1016/j.jcis.2022.04.014](#)
- Lugger SJD, Houben SJA, Foelen Y, Debije MG, Schenning APHJ, Mulder DJ. Hydrogen-bonded Supramolecular liquid Crystal Polymers: smart Materials with Stimuli-Responsive, Self-Healing, and recyclable Properties. *Chem Rev.* 2022;122(5):4946–4975. doi:[10.1021/acs.chemrev.1c00330](#)
- Chen L, Sheng X, Li G, Huang F. Mechanically interlocked polymers based on rotaxanes. *Chem Soc Rev.* 2022;51(16):7046–7065. doi:[10.1039/D2CS00202G](#)
- Lee M, Choi I, Kim A, Paik S, Kim D, Kim H, Nam KW. Supramolecular Metal-organic Framework for the high Stability of aqueous Rechargeable zinc Batteries. *ACS Nano.* 2024;18(33):22586–22595. doi:[10.1021/acsnano.4c08550](#)
- Sun P, Qin B, Xu JF, Zhang X. Supramonomers for controllable supramolecular polymerization and renewable supramolecular polymeric materials. *Prog Polym Sci.* 2022;124:101486. doi:[10.1016/j.progpolymsci.2021.101486](#)
- Wang Z, Sun C, Yang K, Chen X, Wang R. Cucurbituril-based Supramolecular polymers for biomedical Applications. *Angew Chem Int Ed.* 2022;61(38):202206763. doi:[10.1002/anie.202206763](#)
- Han W, Xiang W, Li Q, Zhang H, Yang Y, Shi J, Ji Y, Wang S, Ji X, Khashab NM, Sessler JL. Water compatible supramolecular polymers: recent progress. *Chem Soc Rev.* 2021;50(18):10025–10043. doi:[10.1039/D1CS00187F](#)
- Chen J, Zhang Y, Zhao L, Zhang Y, Chen L, Ma M, Du X, Meng Z, Li C, Meng Q. Supramolecular drug Delivery system from Macrocyclic-based Self-assembled Amphiphiles for effective Tumor Therapy. *ACS Appl Mater & Interfaces.* 2021;13(45):53564–53573. doi:[10.1021/acsami.1c14385](#)
- Shurpik DN, Makhmutova LI, Usachev KS, Islamov DR, Mostovaya OA, Nazarova AA, Kizhnyayev VN, Stoikov II. Towards universal Stimuli-responsive Drug delivery Systems: Pillar[5]arenes synthesis and Self-assembly into nanocontainers with tetrazole Polymers. *Nanomaterials.* 2021;11(4):947. doi:[10.3390/nano11040947](#)
- Liu X, Sun X, Liang G. Peptide-based supramolecular hydrogels for bioimaging applications. *Biomater Sci.* 2020;9(2):315–327. doi:[10.1039/D0BM01020K](#)
- Sato K, Muraoka T, Kinbara K. Supramolecular transmembrane Ion channels Formed by multiblock Amphiphiles. *Acc Chem Res.* 2021;54(19):3700–3709. doi:[10.1021/acs.accounts.1c00397](#)
- Rodon-Fores J, Würbser MA, Kretschmer M, Rieß B, Bergmann AM, Lieleg O, Boekhoven J. A chemically fueled supramolecular glue for self-healing gels. *Chem Sci.* 2022;13(38):11411–11421. doi:[10.1039/D2SC03691F](#)
- Jeon WS, Moon K, Park SH, Chun H, Ko YH, Lee JY, Lee ES, Samal S, Selvapalam N, Rekharsky MV, Sindelar V, Sobransingh D, Inoue Y, Kaifer AE, Kim K. Complexation of ferrocene Derivatives by the Cucurbit[7]uril Host: A comparative Study of the cucurbituril and cyclodextrin Host Families. *J Am Chem Soc.* 2005;127(37):12984–12989. doi:[10.1021/ja052912c](#)
- Hartgerink JD, Beniash E, Stupp SI. Self-assembly and mineralization of Peptide-amphiphile Nanofibers. *Science.* 2001;294(5547):1684–1688. doi:[10.1126/science.1063187](#)
- Zhang W, Jin W, Fukushima T, Saeki A, Seki S, Aida T. Supramolecular linear Heterojunction composed of Graphite-like Semiconducting nanotubular Segments. *Science.* 2011;334(6054):340–343. doi:[10.1126/science.1210369](#)
- Ogoshi T, Kanai S, Fujinami S, Yamagishi T, Nakamoto Y. para-bridged Symmetrical Pillar[5]arenes: their Lewis acid Catalyzed synthesis and Host-guest Property. *J Am Chem Soc.* 2008;130(15):5022–5023. doi:[10.1021/ja711260m](#)
- Kursunlu AN, Bastug E, Oguz A, Oguz M, Yilmaz M. A highly branched macrocycle-based dual-channel sensor: bodipy and pillar[5]arene combination for detection of Sn (II) & Hg (II) and bioimaging in living cells. *Anal Chim Acta.* 2022;1196:339542. doi:[10.1016/j.aca.2022.339542](#)
- Gómez-González B, García-Río L, Basilio N, Mejuto JC, Simal-Gandara J. Molecular recognition by Pillar[5]arenes: evidence

- for simultaneous Electrostatic and hydrophobic Interactions. *Pharmaceutics*. 2021;14(1):60. doi:[10.3390/pharmaceutics14010060](https://doi.org/10.3390/pharmaceutics14010060)
21. Shangguan L, Chen Q, Shi B, Huang F. Enhancing the solubility and bioactivity of anticancer drug tamoxifen by water-soluble pillar[6]arene-based host-guest complexation. *Chem Commun*. 2017;53(70):9749–9752. doi:[10.1039/C7CC05305C](https://doi.org/10.1039/C7CC05305C)
 22. Li YF, Li Z, Lin Q, Yang YW. Functional supramolecular gels based on pillar[n]arene macrocycles. *Nanoscale*. 2019;12(4):2180–2200. doi:[10.1039/C9NR09532B](https://doi.org/10.1039/C9NR09532B)
 23. Li L, Chen R, Hu T, Li Y, Wang Q, He C. Novel magnetic pillar[5]arene polymer as adsorbent for rapid removal of organic pollutants in water or air. *Microchem J*. 2020;153:104524. doi:[10.1016/j.microc.2019.104524](https://doi.org/10.1016/j.microc.2019.104524)
 24. Shurpik DN, Aleksandrova YI, Mostovaya OA, Nazmutdinova VA, Zelenikhin PV, Subakaeva EV, Mukhametzyanov TA, Cragg PJ, Stoikov II. Water-soluble pillar[5]arene sulfo-derivatives self-assemble into biocompatible nanosystems to stabilize therapeutic proteins. *Bioorganic Chem*. 2021;117:105415. doi:[10.1016/j.bioorg.2021.105415](https://doi.org/10.1016/j.bioorg.2021.105415)
 25. Zhu H, Li Q, Zhu W, Huang F. Pillararenes as versatile Building blocks for fluorescent Materials. *Acc Mater Res*. 2022;3(6):658–668. doi:[10.1021/accountsmr.2c00063](https://doi.org/10.1021/accountsmr.2c00063)
 26. Kosiorek S, Rad N, Sashuk V. Supramolecular catalysis by carboxylated Pillar[n]arenes. *ChemCatChem*. 2020;12(10):2776–2782. doi:[10.1002/cctc.202000082](https://doi.org/10.1002/cctc.202000082)
 27. Shamagsumova RV, Shurpik DN, Padnya PL, Stoikov II, Evtugyn GA. Acetylcholinesterase biosensor for inhibitor measurements based on glassy carbon electrode modified with carbon black and pillar[5]arene. *Talanta*. 2015;144:559–568. doi:[10.1016/j.talanta.2015.07.008](https://doi.org/10.1016/j.talanta.2015.07.008)
 28. Mei Y, Zhang QW, Gu Q, Liu Z, He X, Tian Y. Pillar[5]arene-based Fluorescent sensor Array for biosensing of intracellular Multi-neurotransmitters through Host-guest Recognitions. *J Am Chem Soc*. 2022;144(5):2351–2359. doi:[10.1021/jacs.1c12959](https://doi.org/10.1021/jacs.1c12959)
 29. Wang J, Guo X, Zhou Q, Cai Y, Lu B, Wang Y, Yao Y. Pillar[5]arene functionalized au NPs and BiOX (Cl/Br/I) heterojunction constructed the enhanced photo-electrochemical sensor for ultrasensitive detection of serotonin. *Colloids Surf A: Physicochem Eng Asp*. 2024;688:133511. doi:[10.1016/j.colsurfa.2024.133511](https://doi.org/10.1016/j.colsurfa.2024.133511)
 30. Zhang YF, Wang ZH, Yao XQ, Zhang YM, Wei TB, Yao H, Lin Q. Novel tripodal-pillar[5]arene-based chemical sensor for efficient detection and removal paraquat by synergistic effect. *Sens Actuators B: Chem*. 2021;327:128885. doi:[10.1016/j.snb.2020.128885](https://doi.org/10.1016/j.snb.2020.128885)
 31. Yu D, Deng W, Wei X. Supramolecular aggregate of pillar[5]arene-based Cu(II) coordination complexes as a highly selective fluorescence sensor for nitroaromatics and metal ions. *Dyes Pigments*. 2023;210:110968. doi:[10.1016/j.dyepig.2022.110968](https://doi.org/10.1016/j.dyepig.2022.110968)
 32. Yu S, Wang Y, Chatterjee S, Liang F, Zhu F, Li H. Pillar[5]arene-functionalized nanochannel platform for detecting chiral drugs. *Chin Chem Lett*. 2021;32(1):179–183. doi:[10.1016/j.cclet.2020.11.055](https://doi.org/10.1016/j.cclet.2020.11.055)
 33. Wang J, Zhou L, Bei J, Zhao Q, Li X, He J, Cai Y, Chen T, Du Y, Yao Y. An enhanced photo-electrochemical sensor constructed from pillar[5]arene functionalized au NPs for ultrasensitive detection of caffeic acid. *Talanta*. 2022;243:123322. doi:[10.1016/j.talanta.2022.123322](https://doi.org/10.1016/j.talanta.2022.123322)
 34. Smolko V, Shurpik D, Porfireva A, Evtugyn G, Stoikov I, Hianik T. Electrochemical aptasensor Based on Poly(neutral Red) and carboxylated Pillar[5]arene for sensitive Determination of aflatoxin M1. *Electroanalysis*. 2018;30(3):486–496. doi:[10.1002/elan.201700735](https://doi.org/10.1002/elan.201700735)
 35. Stoikov D, Shafigullina I, Shurpik D, Stoikov I, Evtugyn G. A Flow-through Biosensor system Based on Pillar[3]Arene[2]quinone and ferrocene for determination of hydrogen Peroxide and uric Acid. *Chemosensors*. 2024;12(6):98. doi:[10.3390/chemosensors12060098](https://doi.org/10.3390/chemosensors12060098)
 36. Stoikov DI, Porfir'eva AV, Shurpik DN, Stoikov II, Evtugyn GA. Electrochemical DNA sensors on the basis of electropolymerized thionine and azure B with addition of pillar[5]arene as an electron transfer mediator. *Russ Chem Bull*. 2019;68(2):431–437. doi:[10.1007/s11172-019-2404-8](https://doi.org/10.1007/s11172-019-2404-8)
 37. Podeh MRH, Bhattacharya SK, Qu M. Effects of nitrophenols on acetate utilizing methanogenic systems. *Water Res*. 1995;29(2):391–399. doi:[10.1016/0043-1354\(94\)00193-B](https://doi.org/10.1016/0043-1354(94)00193-B)
 38. Shi Q, Chen M, Diao G. Electrocatalytic reduction of m-nitrophenol on reduced graphene oxide modified glassy carbon electrode. *Electrochim Acta*. 2013;114:693–699. doi:[10.1016/j.electacta.2013.10.108](https://doi.org/10.1016/j.electacta.2013.10.108)
 39. Boddu V, Kim S, Adkins J, Weimer E, Paul T, Damavarapu R. Sensitive determination of nitrophenol isomers by reverse-phase high-performance liquid chromatography in conjunction with liquid-liquid extraction. *Int J Environ Anal Chem*. 2017;97(11):1053–1064. doi:[10.1080/03067319.2017.1381235](https://doi.org/10.1080/03067319.2017.1381235)
 40. Qu F, Chen P, Zhu S, You J. High selectivity of colorimetric detection of p-nitrophenol based on ag nanoclusters. *Spectrochim Acta Part A: Mol Biomol Spectrosc*. 2017;171:449–453. doi:[10.1016/j.saa.2016.08.043](https://doi.org/10.1016/j.saa.2016.08.043)
 41. Khan KO, Assiri MA, Irshad H, Rafique S, Khan AM, Khan AK, Imran M, Shahzad SA. Fluorescence based detection of industrially important and hazardous 4-nitrophenol in real Samples: A combination of extensive optical and theoretical studies. *J Photochem Photobiol A: Chem*. 2023;442:114805. doi:[10.1016/j.jphotochem.2023.114805](https://doi.org/10.1016/j.jphotochem.2023.114805)
 42. ALOthman ZA, Badjah AY, Locatelli M, Ali I. Multi-walled Carbon nanotubes Solid-phase Extraction and capillary Electrophoresis methods for the analysis of 4-cyanophenol and 3-nitrophenol in Water. *Molecules*. 2020;25(17):3893. doi:[10.3390/molecules25173893](https://doi.org/10.3390/molecules25173893)
 43. Cheng XL, Xia X, Xu QQ, Wang J, Sun JC, Zhang Y, Li SS. Superior conductivity FeSe₂ for highly sensitive electrochemical detection of p-nitrophenol and o-nitrophenol based on synergistic effect of adsorption and catalysis. *Sens Actuators B: Chem*. 2021;348:130692. doi:[10.1016/j.snb.2021.130692](https://doi.org/10.1016/j.snb.2021.130692)
 44. He Q, Wang B, Liang J, Liu J, Liang B, Li G, Long Y, Zhang G, Liu H. Research on the construction of portable electrochemical sensors for environmental compounds quality monitoring. *Mater Today Adv*. 2023;17:100340. doi:[10.1016/j.mtadv.2022.100340](https://doi.org/10.1016/j.mtadv.2022.100340)
 45. Shamagsumova RV, Kulikova TN, Porfireva AV, Shurpik DN, Stoikov II, Rogov AM, Stoikov DI, Evtugyn GA. Electrochemistry and electrochemical assessment of host-guest complexation of substituted pillar[m]arene[n]quinones. *J Electroanal Chem*. 2023;938:117444. doi:[10.1016/j.jelechem.2023.117444](https://doi.org/10.1016/j.jelechem.2023.117444)
 46. SanPiN 2.1.7.573-96. Sanitarnye pravila i normy 2.1.7. POChVA, ochistka naseleennyh mest, bytovye i promyshlennyye otdohy, sanitarnaya ohrana pochvy. Gigienicheskie trebovaniya k ispol'zovaniyu stochnyh vod i ih osadkov dlya orosheniya i udobreniya. Prilozhenie 1 [SanPiN 2.1.7.573-96. Sanitary rules and regulations 2.1.7. SOIL, cleaning of populated areas, household and industrial waste, sanitary protection of soil. Hygienic requirements for the use of wastewater and its sediments for irrigation and fertilization. Supplement 1]. Moscow: Informacionno-izdatel'skiy centr Minzdrava Rossii; 1997. 54 p. Russian.
 47. Kappo D, Kuzin YI, Shurpik DN, Stoikov II, Evtugyn GA. Voltammetric DNA sensor Based on Redox-active Dyes for determining Doxorubicin. *J Anal Chem*. 2022;77(1):94–100. doi:[10.1134/S1061934822010075](https://doi.org/10.1134/S1061934822010075)
 48. Makhmutova LI, Shurpik DN, Mostovaya OA, Lachugina NR, Gerasimov AV, Guseinova A, Evtugyn GA, Stoikov II. A supramolecular electrochemical probe based on a tetrazole derivative pillar[5]arene/methylene blue system. *Org & Biomol Chem*. 2024;22(21):4353–4363. doi:[10.1039/D4OB00591K](https://doi.org/10.1039/D4OB00591K)
 49. Smolko V, Shurpik D, Evtugyn V, Stoikov I, Evtugyn G. Organic acid and DNA sensing with electrochemical sensor based on carbon Black and Pillar[5]arene. *Electroanalysis*. 2016;28(6):1391–1400. doi:[10.1002/elan.201501080](https://doi.org/10.1002/elan.201501080)

50. Smolko VA, Shurpik DN, Shamagsumova RV, Porfireva AV, Evtugyn VG, Yakimova LS, Stoikov II, Evtugyn GA. Electrochemical behavior of pillar[5]arene on glassy carbon electrode and its interaction with Cu^{2+} and Ag^+ ions. *Electrochim Acta*. 2014;147:726–734. doi:[10.1016/j.electacta.2014.10.007](https://doi.org/10.1016/j.electacta.2014.10.007)
51. Wei T, Huang X, Zeng Q, Wang L. Simultaneous electrochemical determination of nitrophenol isomers with the polyfurfural film modified glassy carbon electrode. *J Electroanal Chem*. 2015;743:105–111. doi:[10.1016/j.jelechem.2015.02.031](https://doi.org/10.1016/j.jelechem.2015.02.031)
52. Su R, Tang H, Xi F. Sensitive electrochemical detection of p-nitrophenol by pre-activated glassy carbon electrode integrated with silica nanochannel array film. *Front Chem*. 2022;10:954748. doi:[10.3389/fchem.2022.954748](https://doi.org/10.3389/fchem.2022.954748)
53. Huang R, Liao D, Liu Z, Yu J, Jiang X. Electrostatically assembling 2D hierarchical Nb_2CT_x and zifs-derivatives into Zn-Co-NC nanocage for the electrochemical detection of 4-nitrophenol. *Sens Actuators B: Chem*. 2021;338:129828. doi:[10.1016/j.snb.2021.129828](https://doi.org/10.1016/j.snb.2021.129828)
54. Liu J, Chen Y, Guo Y, Yang F, Cheng F. Electrochemical sensor for o-nitrophenol Based on β -cyclodextrin Functionalized graphene Nanosheets. *J Nanomater*. 2013;2013(1):1–6. doi:[10.1155/2013/632809](https://doi.org/10.1155/2013/632809)
55. Arfin T, Bushra R, Mohammad F. Electrochemical sensor for the sensitive detection of o-nitrophenol using graphene oxide-poly(ethyleneimine) dendrimer-modified glassy carbon electrode. *Graphene Technol*. 2016;1(1-4):1–15. doi:[10.1007/s41127-016-0002-1](https://doi.org/10.1007/s41127-016-0002-1)
56. Li C, Wu Z, Yang H, Deng L, Chen X. Reduced graphene oxide-cyclodextrin-chitosan electrochemical sensor: effective and simultaneous determination of o- and p-nitrophenols. *Sens Actuators B: Chem*. 2017;251:446–454. doi:[10.1016/j.snb.2017.05.059](https://doi.org/10.1016/j.snb.2017.05.059)
57. Xu X, Liu Z, Zhang X, Duan S, Xu S, Zhou C. β -cyclodextrin functionalized mesoporous silica for electrochemical selective sensor: simultaneous determination of nitrophenol isomers. *Electrochim Acta*. 2011;58:142–149. doi:[10.1016/j.electacta.2011.09.015](https://doi.org/10.1016/j.electacta.2011.09.015)
58. Ding Z, Zhao J, Hao Z, Guo M, Li L, Li N, Sun X, Zhang P, Cui J. Simultaneous electrochemical determination of nitrophenol isomers based on macroporous carbon functionalized with amino-bridged covalent organic polycalix[4]arenes. *J Hazard Mater*. 2022;423:127034. doi:[10.1016/j.jhazmat.2021.127034](https://doi.org/10.1016/j.jhazmat.2021.127034)
59. Gerent GG, Spinelli A. Magnetite-platinum nanoparticles-modified glassy carbon electrode as electrochemical detector for nitrophenol isomers. *J Hazard Mater*. 2017;330:105–115. doi:[10.1016/j.jhazmat.2017.02.002](https://doi.org/10.1016/j.jhazmat.2017.02.002)
60. He Q, Wang B, Liu J, Li G, Long Y, Zhang G, Liu H. Nickel/nitrogen-doped carbon nanocomposites: synthesis and electrochemical sensor for determination of p-nitrophenol in local environment. *Environ Res*. 2022;214:114007. doi:[10.1016/j.envres.2022.114007](https://doi.org/10.1016/j.envres.2022.114007)
61. Hu C, Pan P, Huang H, Liu H. Cr-MOF-based Electrochemical sensor for the detection of P-Nitrophenol. *Biosensors*. 2022;12(10):813. doi:[10.3390/bios12100813](https://doi.org/10.3390/bios12100813)
62. Li J, Kuang D, Feng Y, Zhang F, Xu Z, Liu M. A graphene oxide-based electrochemical sensor for sensitive determination of 4-nitrophenol. *J Hazard Mater*. 2012;201-202:250–259. doi:[10.1016/j.jhazmat.2011.11.076](https://doi.org/10.1016/j.jhazmat.2011.11.076)
63. Liu Y, Zhu L, Zhang Y, Tang H. Electrochemical sensing of 2,4-dinitrophenol by using composites of graphene oxide with surface molecular imprinted polymer. *Sens Actuators B: Chem*. 2012;171-172:1151–1158. doi:[10.1016/j.snb.2012.06.054](https://doi.org/10.1016/j.snb.2012.06.054)
64. Sangamithirai D, Ramanathan S. Electrochemical sensing platform for the detection of nitroaromatics using g- $\text{C}_3\text{N}_4/\text{V}_2\text{O}_5$ nanocomposites modified glassy carbon electrode. *Electrochim Acta*. 2022;434:141308. doi:[10.1016/j.electacta.2022.141308](https://doi.org/10.1016/j.electacta.2022.141308)
65. Sangamithirai D, Krishna KR, Pandurangan A. Investigating the synergistic effect of RuO_2 nanoparticle-decorated V_2O_5 nanoflakes for sensitive detection of 2,4-dinitrophenol and 2,4-dinitrotoluene. *J. Electroanal. Chem*. 2024;970:118554. doi:[10.1016/j.jelechem.2024.118554](https://doi.org/10.1016/j.jelechem.2024.118554)
66. Faisal M, Alam MM, Ahmed J, Asiri AM, Alsaiani M, Alruwais RS, Madkhali O, Rahman MM, Harraz FA. Efficient detection of 2,6-dinitrophenol with silver Nanoparticle-decorated Chitosan/ SrSnO_3 nanocomposites by differential Pulse Voltammetry. *Biosensors*. 2022;12(11):976. doi:[10.3390/bios12110976](https://doi.org/10.3390/bios12110976)
67. Asiri AM, Adeosun WA, Marwani HM. Electrocatalytic reduction of 2,6-dinitrophenol on polycongo red decorated glassy carbon electrode for sensing application. *J Environ Chem Eng*. 2020;8(5):104378. doi:[10.1016/j.jece.2020.104378](https://doi.org/10.1016/j.jece.2020.104378)
68. Rahman MM, Alam MM, Asiri AM, Chowdhury MA, Uddin J. Electrocatalysis of 2,6-dinitrophenol Based on Wet-chemically Synthesized PbO-ZnO Microstructures. *Catalysts*. 2022;12(7):727. doi:[10.3390/catal12070727](https://doi.org/10.3390/catal12070727)
69. John BK, Thara CR, Korah BK, John N, Mathew B. Bioresource-derived multifunctional carbon quantum dots as a fluorescence and electrochemical sensing platform for picric acid and nontoxic food storage application. *J Ind Eng Chem*. 2023;126:546–556. doi:[10.1016/j.jiec.2023.06.043](https://doi.org/10.1016/j.jiec.2023.06.043)
70. Karthika P, Shanmuganathan S, Viswanathan S. Electrochemical sensor for picric acid by using molecularly imprinted polymer and reduced graphene oxide modified pencil graphite electrode. *Proc Indian National Sci Acad*. 2022;88(3):263–276. doi:[10.1007/s43538-022-00084-3](https://doi.org/10.1007/s43538-022-00084-3)
71. Wang Y, Cao W, Wang L, Zhuang Q, Ni Y. Electrochemical determination of 2,4,6-trinitrophenol using a hybrid film composed of a copper-based metal organic framework and electroreduced graphene oxide. *Microchim Acta*. 2018; 185(6):315. doi:[10.1007/s00604-018-2857-8](https://doi.org/10.1007/s00604-018-2857-8)
72. Gigenicheskie normativy GN 2.1.5.1315-03. Predel'no dopustimye koncentracii (PDK) himicheskikh veshchestv v vode vodnykh ob"ektov hozyajstvenno-pit'evogo i kul'turno-bytovogo vodopol'zovaniya [Hygienic Regulations HR 2.1.5.1315-03. Maximum permissible concentrations (MPC) of chemicals in the water of water objects of economic, drinking and cultural water use]. Moscow: Russian Register of Potentially Hazardous Chemical and Biological Substances of the Ministry of Health of the Russian Federation; 2003. 154 p. Russian.